Hindawi
Advances in Materials Science and Engineering
Volume 2018, Article ID 5153041, 8 pages
https://doi.org/10.1155/2018/5153041

Research Article

Self-Healing of Concrete Cracks by Ceramsite-Loaded Microorganisms

Jing Xu,[1] Xianzhi Wang,[1] Junqing Zuo ,[2] and Xiaoyan Liu [3]

[1] *Key Laboratory of Advanced Civil Engineering Materials of the Ministry of Education, Tongji University, Shanghai 201804, China*
[2] *Shanghai Construction Group Co., Ltd., Shanghai 200080, China*
[3] *College of Mechanics and Materials, Hohai University, Nanjing 210098, China*

Correspondence should be addressed to Junqing Zuo; junqingzuo@163.com and Xiaoyan Liu; liuxiaoyan@hhu.edu.cn

Received 15 January 2018; Accepted 2 April 2018; Published 24 June 2018

Academic Editor: Michele Iafisco

Protective carrier is essential for the self-healing of concrete cracks by microbially induced $CaCO_3$ precipitation, owing to the harsh conditions in concrete. In this paper, porous ceramsite particles are used as microbial carrier. Heat treatment and NaOH soaking are first employed to improve the loading content of the ceramsite. The viability of bacterial spores is assessed by urea decomposition measurements. Then, the self-healing efficiency of concrete cracks by spores is evaluated by a series of tests including compressive strength regain, water uptake, and visual inspection of cracks. Results indicate that heat treatment can improve the loading content of ceramsite while not leading to a reduction of concrete strength by the ceramsite addition. The optimal heating temperature is 750°C. Ceramsite particles act as a shelter and protect spores from high-pH environment in concrete. When nutrients and spores are incorporated in ceramsite particles at the same time, nutrients are well accessible to the cells. The regain ratio of the compressive strength increases over 20%, and the water absorption ratio decreases about 30% compared with the control. The healing ratio of cracks reaches 86%, and the maximum crack width healed is near 0.3 mm.

1. Introduction

Since the invention of modern concrete, it has become the most widely used building material all around the world. It stands out for its high compressive strength, low cost, and flexibility in casting. However, durability is the primary concern for concrete engineers. Concrete has a high tendency to cracking, which allows aggressive species to penetrate into the matrix. External loads, temperature gradients, and restrained deformation are the main factors contributing to the crack [1]. Repair of cracks is generally divided into passive and active treatments. For the passive treatment, repair agents are applied to the concrete manually after cracks are detected. This method is very laborsome and costly. For the active treatment, which is also known as self-repair or self-healing, the repair process can be activated upon crack formation without any interferences by human. Besides, cracks could be healed repeatedly in this way [2, 3]. Actually, autogenous healing of concrete itself has already been studied previously. Cracks ranging from 0.1 to 0.3 mm can be fixed though hydration of unhydrated concrete particles, whereas it is very limited [4]. To deal with wider cracks, healing agents in the form of admixtures should be incorporated. Nowadays, more and more researchers consider bio-based agents as a promising candidate.

Bacterial spores, together with nutrients and mineralization precursors, are mixed in concrete mixtures during casting. After hardening, spores will stay as dormant. When the cracks form, bacterial spores are exposed to moisture and air. Then, the spores will rejuvenate and produce minerals, which mostly appear as calcium carbonate, to seal the cracks [1, 5–11]. Meanwhile, the negatively charged cell walls can chelate cations, which makes bacteria cells to act as the nucleation sites of precipitation products. Several types of carbonate-generating pathways had been studied previously. The most common ones are the aerobic respiration and the ureolysis-based types. The former relies on the respiration effects of bacteria to directly convert organic calcium compounds into calcium carbonate [12, 13]. Meanwhile, the latter produces urease as metabolite, which decomposes urea into ammonia and carbon dioxide [1, 4, 14, 15]. With an increase of pH by the hydrolysis of ammonia, a rapid $CaCO_3$ precipitation occurs [16]. In terms of the self-healing efficiency, ureolytic type is much higher due to its high $CaCO_3$ precipitation rate.

In order to allow the bacterially induced concrete self-healing system work, bacterial spores should be incorporated in fresh-state concrete. Basically, there are two ways to add bacterial cells into concrete matrix: directly mixing and carrier immobilization. Directly mixing is much straightforward but will expose bacteria to the harsh environment of concrete, which is harmful to the bacterial activity. Moreover, the process of mixing and continuous hydration could apply physical stress on bacterial cells [17]. According to Jonkers' report, the number of active cells in concrete matrix decreased by 90% after 42 days [1]. Carrier immobilization is a widely used protective method. A variety of carriers, such as porous particles, gels, and microcapsules, can provide a gentle environment for bacteria [14, 18–22]. Carriers should meet the requirements as follows: (1) good compatibility with concrete, (2) relatively high mechanical strength, and (3) high loading content. Intensive studies have been carried out on porous inorganic protective systems which showed quite high healing efficiency due to the fact that the porous inorganic carriers are compatible with concrete matrix and have a high loading content.

For the evaluation of self-healing effects, most of the prior works concentrated on the assessment of crack healing and permeability. The quantitative analysis of the crack width and the ratio of cracks that could be healed was studied. Permeability of concrete, which is a direct reflection of the durability, was evaluated after self-healing [23–26]. However, limited works have been performed on the mechanical properties of concrete before and after bacterially based self-healing. The mechanical behavior of concrete after healing is a vital criterion since most of the concrete is subjected to loading in structures.

In this work, ureolysis-based bacterial spores were applied in mortar to serve as self-healing agents. Compressive tests before and after healing were performed to evaluate the healing effects from the point of mechanics. The efficiency of healing was also studied by crack imaging analysis and water uptake measurements. In order to provide a protection for spores, porous ceramsite particles, which are a type of expanded clay, were employed. Pretreatments on the ceramsite particles were carried out beforehand for the purpose of improving the loading content of the protective carriers.

2. Experimental Details

2.1. Bacterial Strains and Spores Collection. An ureolytic bacterium *Sporosarcina pasteurii* (ATCC11859) was used in this work. Bacterial strains were first rejuvenated by the agar streak method and then cultured in a liquid medium consisting of 5 g peptone, 3 g meat extract, and 20 g urea per liter of distilled water. The medium was sterilized by autoclaving for 20 min at 121°C, and the pH was adjusted to 9. Cultures were aerobically incubated at 30°C in a water bath shaker operated at 100 rpm. Growth was regularly checked quantitatively by the counting method using an optical microscope. After 14 days of incubation, the sporulation achieved more than 90%, and the cells were harvested by centrifugation and resuspension in sterile fresh medium to remove residues. The suspension of the cells was subjected to a pasteurization process of 20 min in a 80°C water bath in order to make sure all the cells were spores. The spore suspension was subsequently kept at 4°C until further use.

2.2. Ceramsite Particle Pretreatment. The porous ceramsite particles were used as protective carriers for bacterial spores and healing agents. The mean particle size was 2–5 mm, and the bulk density was 1036.5 kg/m^3. For the purpose of improving the loading content of ceramsite particles, different pretreatment procedures, such as alkali erosion and sintering treatments, were carried out.

For the alkali erosion treatment, ceramsite particles were first treated by NaOH solution with concentrations of 0.5 mol/L, 1.0 mol/L, and 1.5 mol/L. After immersion in solution for 24 h, ceramsite particles were rinsed repeatedly by distilled water and then oven-dried at 105°C. For the sintering treatment, the selected sintering temperature varied from 400°C to 1000°C. The heating rate was 5°C/min and then kept for 2 h at the maximum temperature, followed by a cooling process in a furnace. After pretreatment, the particles were oven-dried at 105°C and weighed. Then, the loading content was evaluated by immersing the particles in distilled water. After 24 h, particles were taken out, wiped by wet towel to remove water on the surfaces, and weighed. The mass difference before and after immersion was considered as an indicator of loading content.

Considering the possible negative effect of the heating process on the mechanical properties of concrete matrix, compressive strength and flexural strength of concrete matrix with ceramsite treated at different temperatures were determined. For the mechanical tests, $40 \times 40 \times 160$ mm mortar specimens containing 250 g ASTM Type I Ordinary Portland cement, 338 g local natural sand with a specific density of 2.65 g/cm^3, 125 g water, and 196 g ceramsite particles were fabricated. Specimens were cast and cured in a standard curing room at a temperature of 20°C and relative humidity (RH) of 90%. After 24 h, all samples were demolded and then stored in the same room until tests. Triplicate sets for each group were fabricated. The mechanical tests were performed according to standard GB/T 17671-1999.

2.3. Viability of Spores Protected by Ceramsite Loading. Spores were loaded in ceramsite particles by simply immersing 10 g ceramsite in 7.5 mL spore suspension (10^9 cells/mL) for 2 h. Then the particles were dried in an oven at 40°C until the weight remains constant. The viability of spores with or without the protection from ceramsite was evaluated by a treatment in a simulated concrete pore

Table 1: The mixing proportion.

Group	Cement (g)	Sand (g)	Water (g)	Ceramsite (g)	Beef extract (g)	Peptone (g)	Urea (g)	Calcium nitrate (g)	Basalt fiber (g)	Water-reducing agent (g)
C	250	338	125	196[a]	—	—	—	—	8	1.0
N	250	338	125	197.6[b]	—	—	2.5	1.5	8	1.2
S	250	338	125	197[c]	0.3	0.5	2.5	1.5	8	1.2
SN	250	338	125	197.5[d]	—	—	2.5	1.5	8	1.2

Note: [a]ceramsite without loading; [b]ceramsite loaded with 0.6 g beef extract and 1 g peptone; [c]ceramsite loaded with 1 g spores; [d]ceramsite loaded with 0.3 g beef extract, 0.5 g peptone, and 0.7 g spores.

solution. The solution was prepared by mixing cement (the same as described in Section 2.2) and water at a large water-to-cement (w/c) ratio of 10. Cement was first mixed with water in a 100 ml falcon tube and then put into a shaker at 100 rpm for 1 h, followed by a filtration procedure.

For the treatment of spores without protection, 1 mL spore suspension (10^9 cells/mL) was mixed with 10 mL simulated solution and left to rest for 24 h. After this, spores were collected by repeated centrifugation and washing by sterile distilled water. For the treatment on loaded spores, 10 g dry ceramsite particles were put into a filtering tea bag, which was then submerged in 10 mL simulated solution for 24 h. After this, the tea bag was taken out and rinsed repeatedly by sterile distilled water. Then, the tea bag was oven-dried at 40°C until the mass remains constant. Ceramsite particles were collected from the opened tea bag.

The amount of urea decomposed by spores was used as an index to evaluate the viability of the spores with or without protection. Urea concentration measurement was based on a colorimetric method as described by Douglas and Bremner [27]. A visible spectrophotometer V-1200 was used for the colorimetric tests. 1 mL spore suspension or 10 g dry ceramsite particles with and without simulated solution treatment were added to 100 mL growth medium, which consists of 5 g peptone, 3 g beef extract, and 20 g urea per liter of distilled water. As a control, an equivalent amount of sterile dry ceramsite particles were added to the same medium. The amount of urea decomposed during 6 days was measured at 20°C. Three replicates were tested in each series.

2.4. Mortar Specimen Preparation and Crack Formation. The cement and sand used were the same as described in Section 2.2. Porous ceramsite particles loaded with nutrients only (group N), spores only (group S), and both spores and nutrients (group SN) were incorporated. Spores together with or without peptone and beef extract were incorporated into porous ceramsite particles by immersing 196 g ceramsite in 150 ml solution dissolved by spores and/or nutrients for 2 h. Then, the particles were dried in an oven at 40°C until the weight remains constant. Besides, ceramsite without loading served as the control group (group C). Urea and calcium nitrate were added directly into the matrix. In order to facilitate the formation of cracks while maintaining the integrity, basalt fibers (TLB Co., China) with a length of 10 mm and diameter of 7 μm were incorporated. The water-reducing agent was also used to regulate the fluidity of the mixture. Table 1 shows the mixing proportion.

Mortar cubes of size $50 \times 50 \times 50$ mm were cast and cured in a standard curing room at a temperature of 20°C and RH of 90%. After 24 h, all samples were demolded and then stored in the same room until tests. Triplicate sets for each group were fabricated.

Cracks were created by a compressive loading program. The compressive tests were performed by using a mechanical testing system (TSY-2000). The displacement control mode was used with a loading rate of 0.1 mm/min. After peak load, the final displacement was controlled in the same way. All specimens were subjected to wet-dry cycles for 4 weeks at 20°C. For one cycle, specimens were submerged in water for 1 h and then exposed to ambient condition (20°C, RH 60%) for 11 h.

2.5. Self-Healing Evaluation. The self-healing effectiveness was evaluated as follows.

2.5.1. Mechanical Tests. The compressive tests were performed using the same mechanical testing system, and the compressive strength of each specimen was recorded. At the same time, cracks were produced. After 28 days healing, compressive strength was tested again under the same circumstance. The strength regain ratio r was defined as the compressive strength of the specimen after healing dividing that of the intact specimen:

$$r = \frac{R_{sh}}{R}, \tag{1}$$

where R is the compressive strength at first loading (MPa) and R_{sh} is the compressive strength after self-healing (MPa).

2.5.2. Water Uptake Tests. Since water uptake is one of the indicators of durability, the capillary water absorption test was performed to evaluate the durability of specimens after self-healing. The mortar cubes were put into the oven at 70°C and dried until their mass loss was less than 0.1% between two measurements at 24 h intervals. After drying, the specimens were then submerged in water, 80 ± 2 mm deep. This was done in an atmosphere of 20°C and an RH of 60%. While the water level was maintained, all specimens were removed from the water every three minutes, dried on the surface with a towel, and weighed. Immediately after this measurement, the specimens were submerged again. The procedure was repeated until weight remains constant.

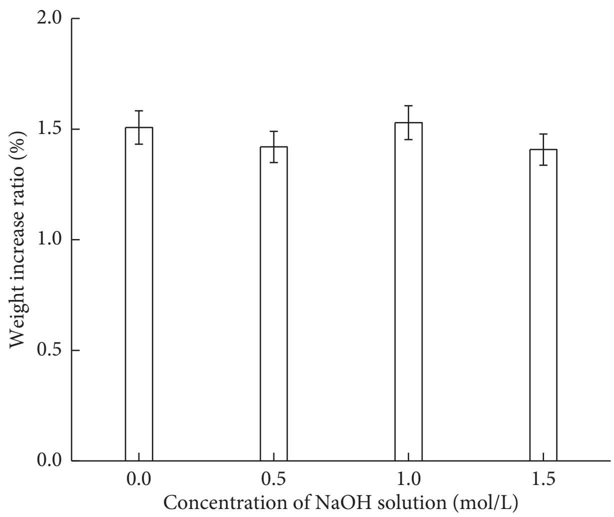

Figure 1: Loading content by alkali erosion at different concentrations of NaOH solution.

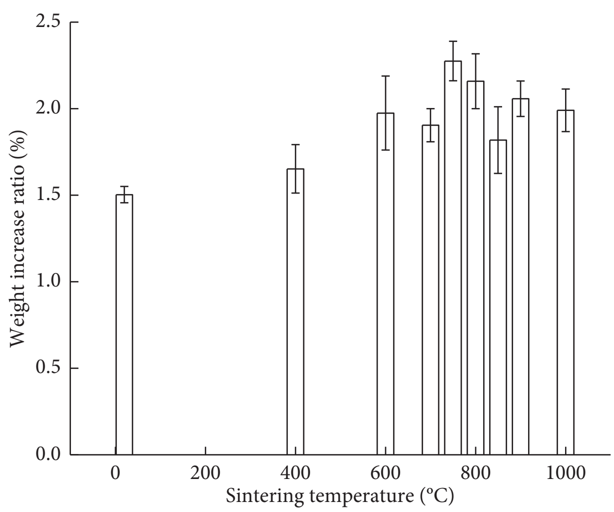

Figure 2: Loading content by heat treatment with different sintering temperatures.

2.5.3. Visual Inspection. Pictures of the sample surfaces were taken before and after self-healing. In each image, crack widths and lengths that can be healed were analyzed by the image processing software "Image J." By setting a threshold value, the cracks can be distinguished from the uncracked area. Thus, the length and width of each crack can be obtained.

3. Results and Discussion

3.1. The Optimal Pretreatment of the Ceramsite. Porosity is positively correlated with the loading content of ceramsite. The main composition of ceramsite is silica. Therefore, alkali erosion by NaOH solution was first considered to increase the porosity of ceramsite particles. Figure 1 shows the effect of alkaline solution treatment on ceramsite. No significant increase of loading content is observed when particles were immersed in NaOH solution with different concentrations, which could possibly due to the fact that the silica of ceramsite is quite inactive in the alkali-silica reaction.

Figure 2 shows the effect of sintering temperature on mass difference. It can be seen that the loading content increased remarkably with increasing sintering temperature, particularly when the temperature was higher than 400°C. However, decrease of loading content is found when the temperature was higher than 800°C. A peak value is observed for sintering temperature of 750°C.

Figure 3 shows the SEM images of ceramsite particles at different sintering temperatures. The pores became wider and open when the temperature increased, especially at 800°C. At higher temperature of 1000°C, pores were closed and the matrix became much denser. As the temperature increased, viscosity of the ceramsite decreased due to the increase in the amount of the vitreous phase. Bloating occurred while small pores fused into larger ones. This phenomenon appeared from 400°C up to 800°C. However, if the temperature rose further, viscosity would decrease excessively, which leads to a shrinkage and condensation of the sintered products and in turn a decreased porosity [28].

Table 2 shows the strength of $40 \times 40 \times 160$ mm prismatic mortar specimens containing ceramsite treated at different temperatures. The compressive strength and flexural strength of specimens containing ceramsite treated at 750°C were 97.79% and 95.97%, respectively, of specimens containing ceramsite without heat treatment. Therefore, it can be concluded that the heat treatment has negligible effect on the mechanical properties of the composites, while the optimal heating temperature is 750°C.

3.2. Viability of Bacterial Spores. The amount of urea decomposed along 6 days, which is an index of bacterial viability, is shown in Figure 4. Free bacterial spores showed the highest ureolytic activity that the urea was degraded completely during 3-4 days. After being treated by a high-alkaline-simulated concrete pore solution, the viability of spores dropped dramatically that urea decomposition could hardly been observed (almost the same as sterile conditions). Loading by ceramsite resulted in a slight decrease of spore viability that a delay of urea decomposition was noticed. This slight viability loss was compensated well under the condition of high-pH treatment because urea could still be completely decomposed after 5 days. Figure 5 shows the SEM images of ceramsite loaded with bacteria spores. A large amount of rod-shaped cells were adsorbed on the surface or in the pores of ceramsite particles. The urea decomposition and SEM imaging tests fully elucidated that porous ceramsite particles provide a preferable microenvironment for the germination and growth of bacterial spores and thus can protect the bacteria from the high-pH condition in concrete.

3.3. Evaluation of Self-Healing Effectiveness. In order to simulate the process of self-healing, cracks were first introduced by compressive loading. After 28 days of incubation, the self-healing effects were evaluated by compressive strength,

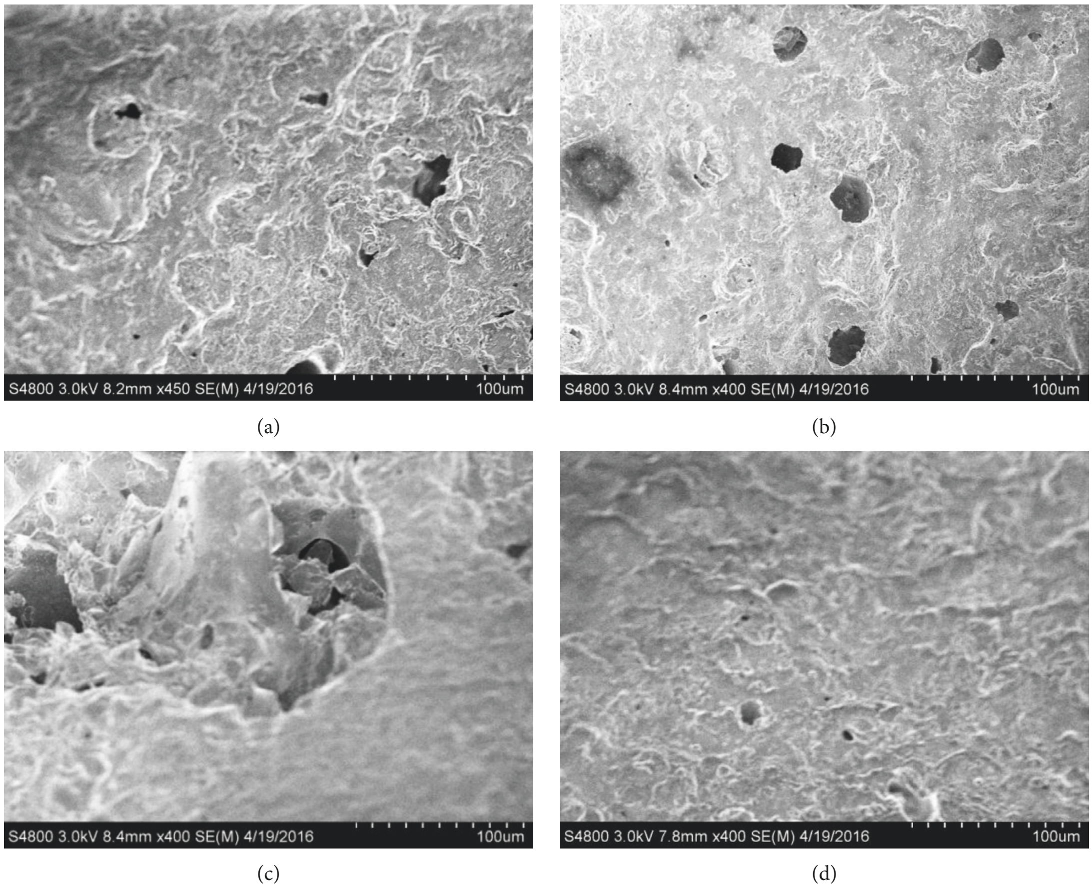

Figure 3: SEM images of ceramsite heated to different temperatures: (a) room temperature; (b) 400°C; (c) 800°C; (d) 1000°C.

Table 2: Strength of mortar specimens containing ceramsite treated at different temperatures.

Mechanical tests	Room temperature	600°C	750°C	900°C
Compressive strength (MPa)	36.39	33.42	35.58	35.68
Flexural strength (MPa)	8.10	8.32	7.77	8.48

water uptake, and image analysis tests. Figure 6 shows the compressive strength regain before and after self-healing. Comparing the regain ratio of the compressive strength values, it is evident that group SN had a much better healing effect than the other groups. After self-healing, the regain ratio of the group SN increased over 20% compared with that of the control group.

Figure 7 shows the water uptake of each group. The capillary water absorption results were consistent with compressive strength, which indicated that the transportation behavior was related to the mechanical properties. All groups had roughly the same pattern. Compared to the control group, the water absorption amount decreased about 30% for the group SN.

Figure 8 shows the crack pattern taken before and after self-healing. Since no obvious $CaCO_3$ precipitation is observed for groups C, N, and S, only pictures of group C are displayed. In contrast, almost all the cracks were sealed and healed by abundant white precipitates for group SN.

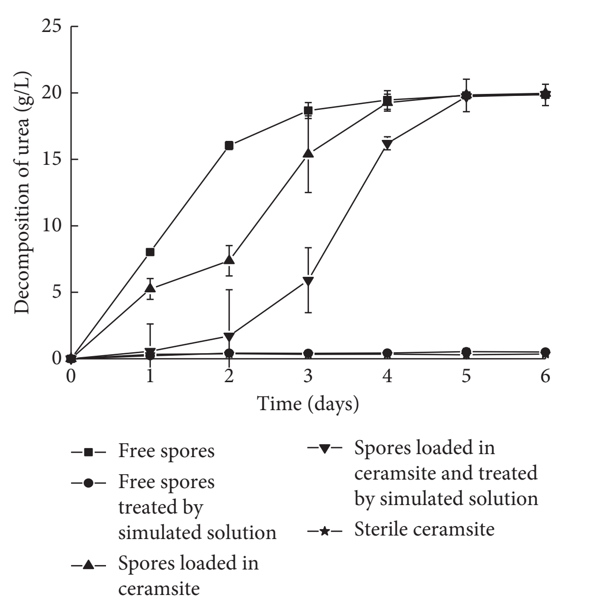

Figure 4: Urea decomposition by free spores and loaded spores with or without treatment by high-pH-simulated solution.

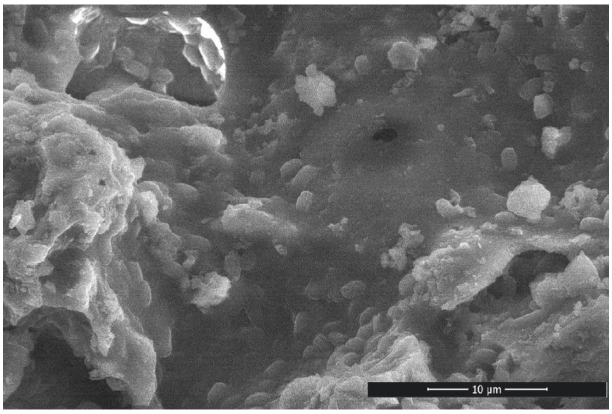

Figure 5: SEM images of spores loaded in ceramsite.

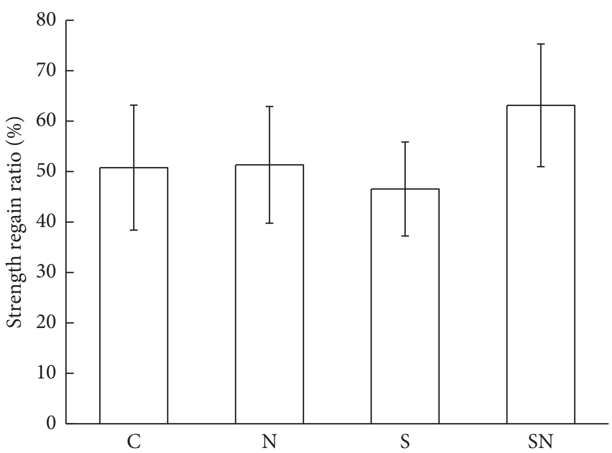

Figure 6: The regain ratio of the compressive strength by self-healing.

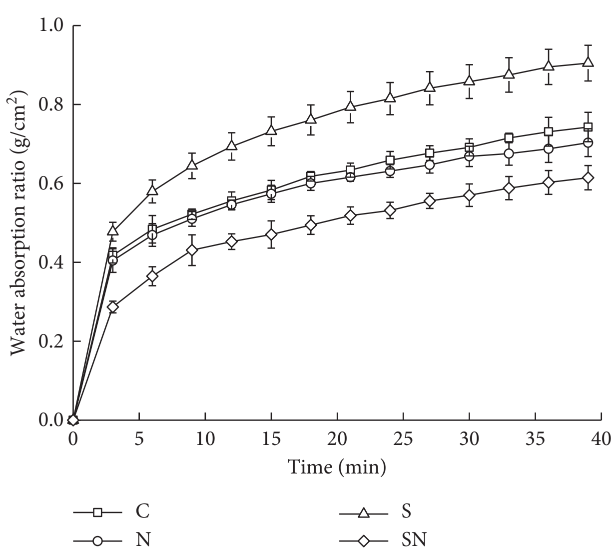

Figure 7: The water uptake after self-healing.

Table 3 shows a summary of the crack healing. The average width and maximum width of cracks that can be healed were around 36 μm and 56 μm for the control group.

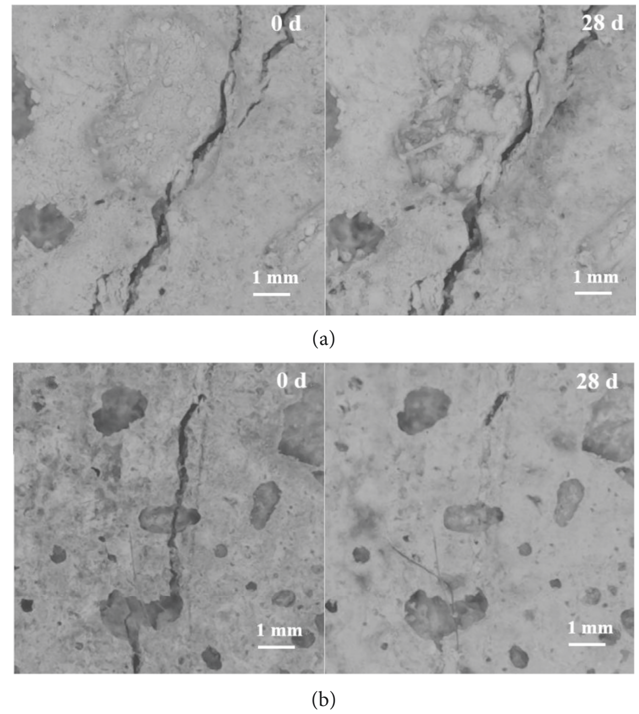

Figure 8: Images of cracks before and after healing: (a) group C; (b) group SN.

Table 3: Summary of the crack healing.

Group	Average healed crack width (μm)	Maximum healed crack width (μm)	Percentage of crack healed
C	36 ± 4	56 ± 4	6 ± 4
N	70 ± 34	124 ± 20	16 ± 11
S	46 ± 15	111 ± 13	7 ± 3
SN	153 ± 58	273 ± 42	86 ± 5

Groups N and S show somewhat better performance than the control group referring to the width of cracks that can be healed; however, the percentage of crack healing was only around 10% among these three groups. Significant enhancement of crack healing efficiency was achieved when bacteria and nutrients were loaded in ceramsite simultaneously. Cracks up to 273 μm can be healed and the crack closure ratio was 86% at the end of 28 days.

For both S and SN groups, bacteria were incorporated in ceramsite and enabled the production of $CaCO_3$, while for C and N groups autogenous healing could occur. We found that the healing effectiveness is highly related to the way of loading. When bacteria were loaded in carriers only, a low healing efficiency, even lower than the control, was observed. This could be owing to the fact that spores instead of live cells were used in the self-healing system. Spores might not be able to germinate without the presence of some organic substances nearby. Besides, some cells could further disintegrate and impair the interfacial region between ceramsite particles and paste matrix. When the organics were loaded in company with bacteria, although the cracks cannot be healed completely, the maximum width of cracks that can be healed was near 0.3 mm. Another benefit was that the negative impact of organic nutrients on the concrete matrix could be avoided if nutrients are loaded in carriers.

4. Conclusions

Heat treatment, instead of NaOH soaking, could increase porosity of ceramsite, which thus improves the immobilization capacity. The optimal heating temperature was 750°C, which results in the highest loading content and a negligible decrease in mechanical strength. Ceramsite particles provide a preferable microenvironment for bacterial spores that the viability of spores can be preserved during the urea decomposition process.

When nutrients and bacterial spores are incorporated into ceramsite particles, nutrients are well accessible to the cells and significant healing effects can be observed. The regain ratio of the compressive strength increased over 20%, and the water absorption ratio decreased about 30% compared with the control. The healing ratio of cracks reaches 86%, and the maximum crack width healed was near 0.3 mm.

Conflicts of Interest

The authors declare that there are no conflicts of interest regarding the publication of this paper.

Acknowledgments

The authors would like to acknowledge the financial support for this study from the National Natural Science Foundation of China (51378011), the Natural Science Foundation of Shanghai (17ZR1441900), and the National Key Research and Development Program of China (2016YFC0700802).

References

[1] H. M. Jonkers, A. Thijssen, G. Muyzer, O. Copuroglu, and E. Schlangen, "Application of bacteria as self-healing agent for the development of sustainable concrete," *Ecological Engineering*, vol. 36, no. 2, pp. 230–235, 2010.

[2] V. C. Li and E. Herbert, "Robust self-healing concrete for sustainable infrastructure," *Journal of Advanced Concrete Technology*, vol. 10, no. 6, pp. 207–218, 2012.

[3] M. Wu, B. Johannesson, and M. Geiker, "A review: self-healing in cementitious materials and engineered cementitious composite as a self-healing material," *Construction and Building Materials*, vol. 28, no. 1, pp. 571–583, 2012.

[4] M. Sahmaran, S. B. Keskin, G. Ozerkan, and I. O. Yaman, "Self-healing of mechanically-loaded self consolidating concretes with high volumes of fly ash," *Cement and Concrete Composites*, vol. 30, no. 10, pp. 872–879, 2008.

[5] W. De Muynck, N. De Belie, and W. Verstraete, "Microbial carbonate precipitation in construction materials: a review," *Ecological Engineering*, vol. 36, no. 2, pp. 118–136, 2010.

[6] L. S. Wong, "Microbial cementation of ureolytic bacteria from the genus Bacillus: a review of the bacterial application on cement-based materials for cleaner production," *Journal of Cleaner Production*, vol. 93, pp. 5–17, 2015.

[7] H. L. Huang, G. Ye, C. X. Qian, and E. Schlangen, "Self-healing in cementitious materials: materials, methods and service conditions," *Materials and Design*, vol. 92, pp. 499–511, 2016.

[8] J. Y. Wang, Y. C. Ersan, N. Boon, and N. De Belie, "Application of microorganisms in concrete: a promising sustainable strategy to improve concrete durability," *Applied Microbiology and Biotechnology*, vol. 100, no. 7, pp. 2993–3007, 2016.

[9] J. Xu and W. Yao, "Multiscale mechanical quantification of self-healing concrete incorporating non-ureolytic bacteria-based healing agent," *Cement and Concrete Research*, vol. 64, no. 1, pp. 1–10, 2014.

[10] V. Achal and A. Mukherjee, "A review of microbial precipitation for sustainable construction," *Construction and Building Materials*, vol. 93, pp. 1224–1235, 2015.

[11] R. Siddique and N. K. Chahal, "Effect of ureolytic bacteria on concrete properties," *Construction and Building Materials*, vol. 25, no. 10, pp. 3791–3801, 2011.

[12] M. Seifan, A. K. Samani, and A. Berenjian, "Bioconcrete: next generation of self-healing concrete," *Applied Microbiology and Biotechnology*, vol. 100, no. 6, pp. 2591–2602, 2016.

[13] J. Xu, W. Yao, and Z. W. Jiang, "Non-ureolytic bacterial carbonate precipitation as a surface treatment strategy on cementitious materials," *Journal of Materials in Civil Engineering*, vol. 26, no. 5, pp. 983–991, 2014.

[14] V. Wiktor and H. M. Jonkers, "Quantification of crack-healing in novel bacteria-based self-healing concrete," *Cement and Concrete Composites*, vol. 33, no. 7, pp. 763–770, 2011.

[15] J. Xu, Y. Du, Z. Jiang, and A. She, "Effects of calcium source on biochemical properties of microbial $CaCO_3$ precipitation," *Frontiers in Microbiology*, vol. 6, pp. 1–7, 2015.

[16] J. Y. Wang, H. Soens, W. Verstraete, and N. De Belie, "Self-healing concrete by use of microencapsulated bacterial spores," *Cement and Concrete Research*, vol. 56, pp. 139–152, 2014.

[17] J. Y. Wang, N. De Belie, and W. Verstraete, "Diatomaceous earth as a protective vehicle for bacteria applied for self-healing concrete," *Journal of Industrial Microbiology & Biotechnology*, vol. 39, no. 4, pp. 567–577, 2012.

[18] S. A. L. de Koster, R. M. Mors, H. W. Nugteren, H. M. Jonkers, G. M. H. Meesters, and J. R. van Ommen, "Geopolymer coating of bacteria-containing granules for use in self-healing concrete," *Procedia Engineering*, vol. 102, pp. 475–484, 2015.

[19] J. Zhang, Y. Liu, T. Feng et al., "Immobilizing bacteria in expanded perlite for the crack self-healing in concrete," *Construction and Building Materials*, vol. 148, pp. 610–617, 2017.

[20] J. L. Zhang, B. X. Mai, T. W. Cai et al., "Optimization of a binary concrete crack self-healing system containing bacteria and oxygen," *Materials*, vol. 10, no. 2, p. 116, 2017.

[21] Z. B. Bundur, M. J. Kirisits, and R. D. Ferron, "Use of pre-wetted lightweight fine expanded shale aggregates as internal nutrient reservoirs for microorganisms in bio-mineralized mortar," *Cement and Concrete Composites*, vol. 84, pp. 167–174, 2017.

[22] H. C. Chen, C. X. Qian, and H. L. Huang, "Self-healing cementitious materials based on bacteria and nutrients immobilized respectively," *Construction and Building Materials*, vol. 126, pp. 297–303, 2016.

[23] F. Pacheco-Torgal and J. A. Labrincha, "Biotech cementitious materials: Some aspects of an innovative approach for concrete with enhanced durability," *Construction and Building Materials*, vol. 40, pp. 1136–1141, 2013.

[24] Y. C. Ersan, E. Hernandez-Sanabria, N. Boon, and N. de Belie, "Enhanced crack closure performance of microbial mortar

through nitrate reduction," *Cement and Concrete Composites*, vol. 70, pp. 159–170, 2016.

[25] M. Luo, C. X. Qian, and R. Y. Li, "Factors affecting crack repairing capacity of bacteria-based self-healing concrete," *Construction and Building Materials*, vol. 87, pp. 1–7, 2015.

[26] H. Ling and C. Qian, "Effects of self-healing cracks in bacterial concrete on the transmission of chloride during electromigration," *Construction and Building Materials*, vol. 144, pp. 406–411, 2017.

[27] L. A. Douglas and J. M. Bremner, "Extraction and colorimetric determination of urea in soils," *Soil Science Society of America Journal*, vol. 34, no. 6, pp. 859–862, 1970.

[28] C. Wang, J.-Z. Wu, and F.-S. Zhang, "Development of porous ceramsite from construction and demolition waste," *Environmental Technology*, vol. 34, no. 15, pp. 2241–2249, 2013.